



Electrochemical Study of Adsorption of 1-H-benzotriazole at Stainless Steel in Hydrochloric Acid Solution Interface as Corrosion Inhibitors

Nazanin Behineh, Mohammad Hossain Zargazi, Hesam Baheri*

Department of Chemistry, Islamic Azad University, Karaj Branch, Karaj

(Received 10 Nov. 2015; Final version received 10 Dec. 2015)

Abstract

The influence of the concentration of 1-H-benzotriazole on the corrosion of 316 stainless steel (SS) in chloride acid 1M solutions was studied. The potentiodynamics polarization and scanning electron microscopy (SEM) have been used. The inhibition efficiency increased with an increase in the concentration of 1-H-benzotriazole. The adsorption of 1-H-benzotriazole onto the SS surface occurs according to the Langmuir isotherm. The corrosion kinetic parameters of 316 stainless steel and thermodynamic adsorption parameters for 1-H-benzotriazole were determined and discussed.

Keywords: *Stainless steel 316, 1-H-benzotriazole, Potentiodynamics polarization, Corrosion inhibition, Kinetic parameters.*

Introduction

Conventional stainless steel 316 has a wide scope of applications in different industries. The corrosion resistance of all types of stainless steel 316 is based on the bilayer structure of the spontaneously formed passive films on their surface in aqueous solutions or in the contact with moist air passive oxide films on stainless steel are usually very thin, consisting primarily of chromium oxide, Cr_2O_3 . The

barrier properties of passive films significantly decrease in the presence of chloride ions, which cause localized corrosion phenomena. Corrosion inhibitors can be used to reduce the corrosion rate of metals exposed to corrosive environments. Schiff base compounds have been previously reported as corrosion inhibitors for copper, aluminum, and steel.

The Schiff base is an organic compound formed by the condensation of an amine and a

*Corresponding author: Hesam Baheri, Department of Chemistry, Islamic Azad University, Karaj Branch, Karaj, Iran. E-mail: h.baheri@kiau.ac.ir

carbonyl group having general formula of $R_1-CH=N-R_2$ where R_1 and R_2 are aryl, alkyl, cycloalkyl or heterocyclic groups. The primary advantages of many Schiff base compounds are that they can be conveniently and easily synthesized from relatively cheap materials and those they are eco-friendly or exhibit low toxicity. The adsorption on the metal surface can be attributed to coordination of the organic compounds via phenol and imines groups. Besides the imines group substitution of different groups also affects the inhibition properties. These compounds in general are adsorbed on the metal surface blocking the active corrosion sites. Inhibition efficiency of an inhibitor depends on the number of adsorption active centers in the molecule and their charge densities, the molecule size, and the mode of adsorption on the metal surface.

The aim of this study is to investigate the inhibition effect of 1-H-benzotriazole on the corrosion of 316 stainless steel (SS) in 1 M chloride solution. Potentiodynamic polarization and scanning electron microscopy (SEM) have been used. The best isotherm has been selected and the effect of the temperature (283–2980K) on the corrosion behaviour of SS in the absence and presence 1-H-benzotriazole have been investigated.

Experimental

Solutions

The electrolytes were prepared using analytical

grade HCl reagents (Merck). The corrosive medium 1 M HCl. All solutions were prepared from double distilled water. The pH of all solutions was 1.5. For each experiment, a freshly made solution was used. All tests were performed in naturally aerated electrolytes.

Materials

The testing material was stainless steel type 316. The steel composition was as follows (in wt.%): C: 0.08, Cr: 18, Ni: 10, Mo: 3.92 and Fe: 68. The structure of 1-H-benzotriazole is given in Figure 1.

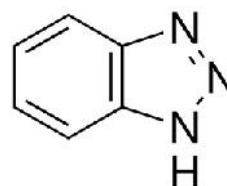


Figure 1. Molecular structure of 1-H-benzotriazole.

The 1-H-benzotriazole is a flat molecule and is stable in air, water and in majority organic solvents. The 1-H-benzotriazole was dissolved at concentrations in the range of 100-500 ppm in chloride solutions, which were mixed with magnetic stirrer.

Electrodes and apparatus

The experiments were carried out in a 200 cm³ glass cell using a three-electrode configuration. The working electrode was prepared from 316 stainless steel rod with rectangular shape which had 4 cm² surface areas. Prior to each experiment the working electrode surface was

treated with 800, 1200, and 2000 grade emery paper, and then thoroughly rinsed with double distilled water. After this the electrode was degreased with ethanol in an ultrasonic bath (~2 min) and then rinsed with double distilled water. The electrode was then immersed in the test electrolyte. Electrode potentials were measured and reported against the external saturated calomel electrode (SCE) connected to the cell via a Luggin probe. A platinum wire was used as a counter electrode. Reference and counter electrodes were individually isolated from the test solution by glass frits. The polarization measurements were performed using an AutoLab PGSTAT 30 potentiostat. The values reported in the paper represent mean values of at least three replicate measurements. Moreover, experiments were carried out at suitably well-chosen temperature ($\pm 0.5^\circ\text{K}$) in an air thermostat with the forced air circulation.

Potentiodynamic experiments

The electrochemical behaviour of 316 stainless steel sample in uninhibited and inhibited solution was studied by recording cathodic and anodic potentiodynamic polarization curves. Before polarization scanning, the electrode potential was changed in range from -800 to 0 mV vs. SCE at a scan rate of 1 mV s^{-1} . The linear Tafel segments of cathodic and anodic curves were extrapolated to corrosion potential (E_{corr}) to obtain corrosion current

densities and the Tafel slopes the cathodic (bc) and anodic (ba) were calculated.

The degree of surface coverage (Θ) and the percentage inhibition efficiency (IE) were calculated from the following equations:

$$\theta = 1 - \frac{j_{\text{corr}}}{j_{\text{corr}}^0} \quad (1)$$

and

$$IE(\%) = \left(\frac{j_{\text{corr}}^0 - j_{\text{corr}}}{j_{\text{corr}}^0} \right) \times 100 \quad (2)$$

Where j_{corr}^0 and j_{corr} are the uninhibited and inhibited corrosion current density values, respectively.

Scanning electron microscopy

The surface morphology of the specimens after immersion in 1M HCl solution in the absence and presence of 1-H-benzotriazole were tested on a Seron Technology-AIS2300C scanning electron microscope (SEM).

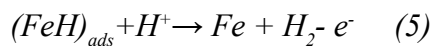
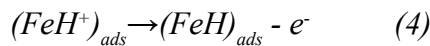
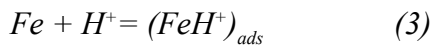
Results and discussion

Potentiodynamic measurements

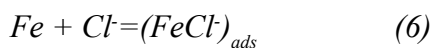
The potentiodynamic behaviours of SS in hydrochloric acid solutions with and without 1-H-benzotriazole at 298°K are shown in Figures 2 and 3 as Tafel plots. The cathodic and anodic current density decreases in the presence of the investigated Schiff base. It shows that the addition of 1-H-benzotriazole molecules reduces the hydrogen evolution reaction and also retards the anodic dissolution

of 316SS.

In hydrochloric acid solutions the following corrosion mechanism of stainless steel is proposed [10,25]. The cathodic hydrogen evaluation:



The anodic dissolution of iron, adsorption tendency of the Cl⁻ ion onto the SS surface according to:



which is similar for (CrCl)_{ads} and (NiCl)_{ads}. However, at more anodic potential the (FeCl)_{ads} layer dissolves onto the surface electrode and the local corrosion of steel occur according to the following reactions:



According to similar reaction from ions of Cr³⁺ and Ni²⁺ ions moreover, for stainless steel the passivation process is possible. Passivity can be defined as a relatively inactive state in which the metal displays a more noble behaviour than thermodynamic conditions predict [26]. The passivation process followed by the production of a thicker oxide film according to the following sequence:

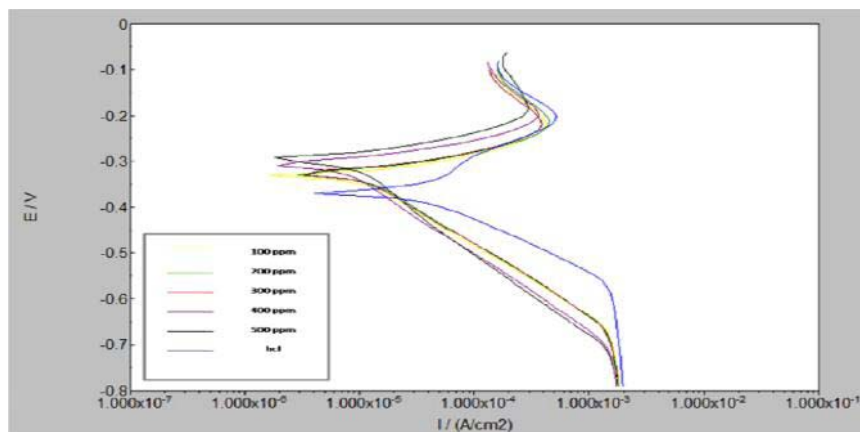
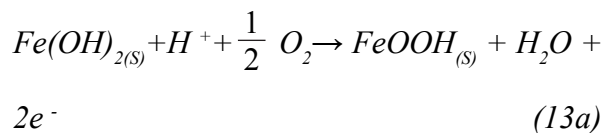
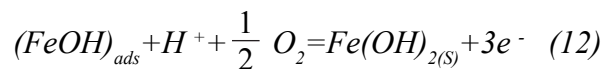
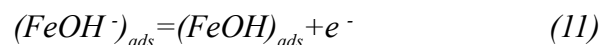
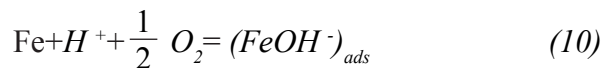


Figure 2. Chosen Tafel plots for 316 stainless steel of 1-H-benzotriazole, dE/dt 1 $mV s^{-1}$, at temperature 298⁰K.

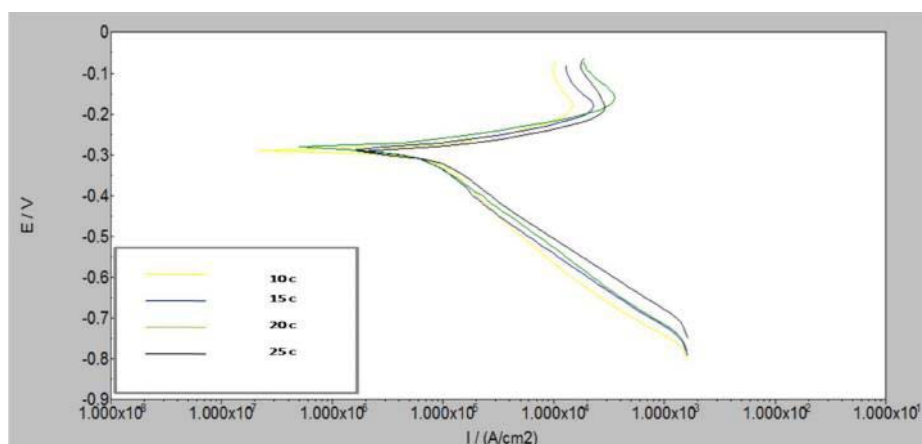
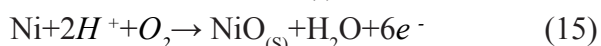
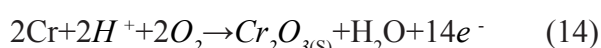


Figure 3. Tafel plots for 316 stainless steel. Solution containing 1 M HCl and 500 ppm of 1-H-benzotriazole, at temperatures 283, 288, 293, 298⁰K dE/dt 1 mV s⁻¹.

Or:



Moreover, formation of a passive layer can be enriched as a result of following oxides:



Which is concern to products of reaction which were placed on the surface of electrode. However, at more anodic potential dissolves the passive layer onto the surface electrode. This means that a passive film on stainless steel is formed even in the acid medium which is a poor electroconductor for which formation and thickening were mainly caused by ionic conductance [27]. The effect of temperature was evaluated by polarization curves test at different temperatures in acid chloride solutions in absence and presence

of 1-H-benzotriazole, Figure 4. As seen in Figure 4 the cathodic and anodic current density increases with an increase in the temperature of solution.

Corrosion parameters i.e. corrosion potential (E_{corr}), cathodic and anodic Tafel slopes (b_c) and (b_a), and corrosion current density (j_{corr}) obtained from the Tafel extrapolation method of the polarization curves are given in Table1. It should be noted that E_{corr} shifted towards more positive values with an increase in the temperature and concentration of 1-H-benzotriazole. A compound can be classified as a cathodic or an anodic type inhibitor when the change in the E_{corr} values is larger than ± 85 mV with respect to the corrosion potential of the blank [28].

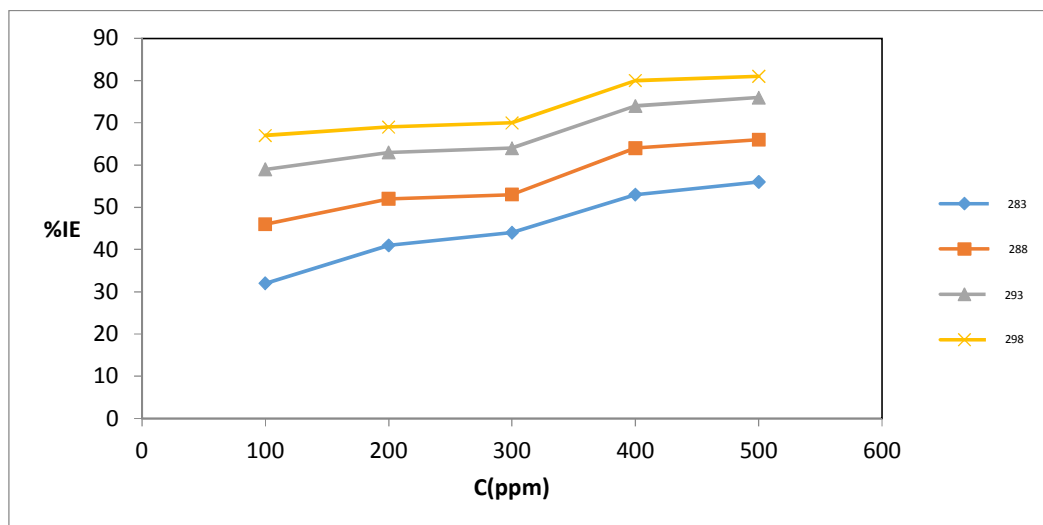


Figure 4. Corrosion inhibition efficiency for 316 stainless steel in a 1 M HCl solution in the presence of 1-H-benzotriazole, at temperatures: (a) 283, (b) 288, (c) 293, (d) 298^oK.

Since the largest displacement exhibited by 1-H-benzotriazole were about 40 mV at different temperature of solutions (Table 1). It may be concluded that of 1-H-benzotriazole in acid chloride environment should be considered as a mixed-type inhibitor. Moreover, the cathodic (b_c) and anodic (b_a) Tafel slopes (Table 1) of 1-H-benzotriazole were found to change with temperatures and inhibitor concentration, this indicates that of 1-H-benzotriazole affected both of these reactions [29]. Results presented in Table 1 show that an increase in temperature increases the corrosion current density, while the addition of 1-H-benzotriazole decreases the j_{corr} values as compared to the control (blank) values across the temperature range indicates the inhibiting effect of Schiff base.

The degree of surface coverage was calculated from the Equation (1). The results (Table 1) showed that the Θ increased

with in temperature and the concentration of 1-H-benzotriazole. Consequently, the corrosion inhibition efficiency can also be calculated from polarization tests by using the Equation (2) the values IE are presented in Figure 5. The inhibition efficiency increases with an increase both concentration (especially for small concentration) of inhibitor, and temperature of the solution. Such behaviour of 1-H-benzotriazole proves about strong adsorption of 1-H-benzotriazole onto the 316 stainless steel surface. Adsorption is the mechanism generally accepted to explain the inhibitory action of organic corrosion inhibitors. The adsorption of inhibitors can affect the corrosion process in two ways: (i) by decreasing the available reaction area (geometric blocking effect), and (ii) by modifying the activation energy of the cathodic and/or anodic reactions [30]. This problem will be discussed in the next part of the work.

Table 1. Corrosion parameters for 316 stainless steel in a 1 M HCl in the absence and presence of 1-H-benzotriazole, and corresponding degree of surface coverage at different temperatures.

| Temperatures | C (ppm) | -E _{cor} (mv) | I _{cor} (mA/cm ²) | bc mv/dec | ba mv/dec | Corr. rate mm/year | θ | %IE |
|--------------|------------|---------------------------|---|--------------|--------------|--------------------------|-------|-----|
| 283 | Blank | 335 | 3.568 × 10 ⁻³ | 134 | 101 | 4.144 × 10 ⁻² | - | - |
| | 100 | 296 | 2.423 × 10 ⁻³ | 218 | 62 | 2.814 × 10 ⁻² | 0.320 | 32 |
| | 200 | 284 | 2.113 × 10 ⁻³ | 243 | 53 | 2.454 × 10 ⁻² | 0.407 | 41 |
| | 300 | 294 | 1.996 × 10 ⁻³ | 220 | 58 | 2.318 × 10 ⁻² | 0.440 | 44 |
| | 400 | 273 | 1.689 × 10 ⁻³ | 229 | 53 | 1.962 × 10 ⁻² | 0.526 | 53 |
| | 500 | 287 | 1.571 × 10 ⁻³ | 229 | 58 | 1.824 × 10 ⁻² | 0.559 | 56 |
| 288 | Blank | 326 | 4.807 × 10 ⁻³ | 135 | 104 | 5.584 × 10 ⁻² | - | - |
| | 100 | 291 | 2.589 × 10 ⁻³ | 279 | 66 | 3.007 × 10 ⁻² | 0.461 | 46 |
| | 200 | 287 | 2.324 × 10 ⁻³ | 214 | 54 | 2.699 × 10 ⁻² | 0.516 | 52 |
| | 300 | 281 | 2.238 × 10 ⁻³ | 267 | 57 | 2.271 × 10 ⁻² | 0.534 | 53 |
| | 400 | 283 | 1.746 × 10 ⁻³ | 209 | 49 | 2.028 × 10 ⁻² | 0.636 | 64 |
| | 500 | 285 | 1.618 × 10 ⁻³ | 204 | 66 | 1.879 × 10 ⁻² | 0.663 | 66 |
| 293 | Blank | 350 | 6.905 × 10 ⁻³ | 128 | 126 | 8.019 × 10 ⁻² | - | - |
| | 100 | 324 | 2.791 × 10 ⁻³ | 159 | 52 | 3.241 × 10 ⁻² | 0.595 | 59 |
| | 200 | 283 | 2.552 × 10 ⁻³ | 230 | 64 | 2.964 × 10 ⁻² | 0.630 | 63 |
| | 300 | 296 | 2.469 × 10 ⁻³ | 216 | 64 | 2.868 × 10 ⁻² | 0.642 | 64 |
| | 400 | 275 | 1.794 × 10 ⁻³ | 244 | 75 | 2.083 × 10 ⁻² | 0.740 | 74 |
| | 500 | 282 | 1.661 × 10 ⁻³ | 208 | 57 | 1.929 × 10 ⁻² | 0.759 | 76 |
| 298 | Blank | 368 | 9.139 × 10 ⁻³ | 121 | 145 | 1.061 × 10 ⁻¹ | - | - |
| | 100 | 332 | 2.955 × 10 ⁻³ | 162 | 53 | 3.479 × 10 ⁻² | 0.672 | 67 |
| | 200 | 325 | 2.816 × 10 ⁻³ | 164 | 46 | 3.271 × 10 ⁻² | 0.691 | 69 |
| | 300 | 324 | 2.736 × 10 ⁻³ | 158 | 52 | 3.177 × 10 ⁻² | 0.700 | 70 |
| | 400 | 304 | 1.844 × 10 ⁻³ | 171 | 48 | 2.141 × 10 ⁻² | 0.798 | 80 |
| | 500 | 294 | 1.706 × 10 ⁻³ | 180 | 50 | 1.982 × 10 ⁻² | 0.813 | 81 |

Activation parameters

Thermodynamic activation parameters have an important role in understanding the inhibitive mechanism of organic inhibitors. Activation parameters such as: the activation of energies (E_a), the enthalpy of activation (ΔH_a), and the

entropy of activation (ΔS_a) were calculated from an Arrhenius-type plot [30,31]:

$$j_{Corr} = A \exp\left(\frac{-E_a}{RT}\right) \quad (16)$$

And transition-state :

$$j_{corr} = \left(\frac{RT}{Nh}\right) \exp\left(\frac{\Delta S_a}{R}\right) \exp\left(\frac{-\Delta S_a}{RT}\right) \quad (17)$$

where A is the Arrhenius constant, N is

the Avogadro's constant, h is the Planck's constant, T is the absolute temperature, R is the universal gas constant, and

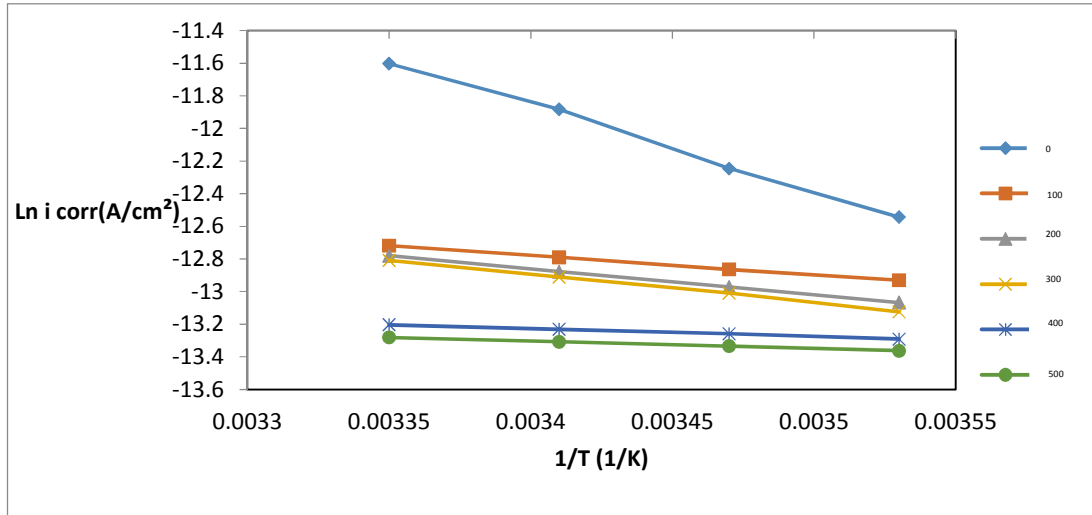


Figure 5. Arrhenius plots for 316 stainless steel. Solution containing 1 M HCl as well as: 0, 100, 200, 300, 400, 500ppm of 1-H-benzotriazole.

Plots of $\ln(j_{\text{corr}})$ vs. $1/T$, Figure 6, and $\ln(j_{\text{corr}}/T)$ vs. $1/T$, Figure 7 give straight lines with slopes of $-E_a/R$, and $-\Delta H_a/R$ respectively. Corrosion kinetic parameters for the SS obtained from these graphs are given in Table 2. The value the energy of activation was higher for uninhibited solution (44 kJ mol^{-1}), than in presence of Schiff base (3.7 kJ mol^{-1}). The lower activation energy in the presence of inhibitor is indication for its chemisorption [13].

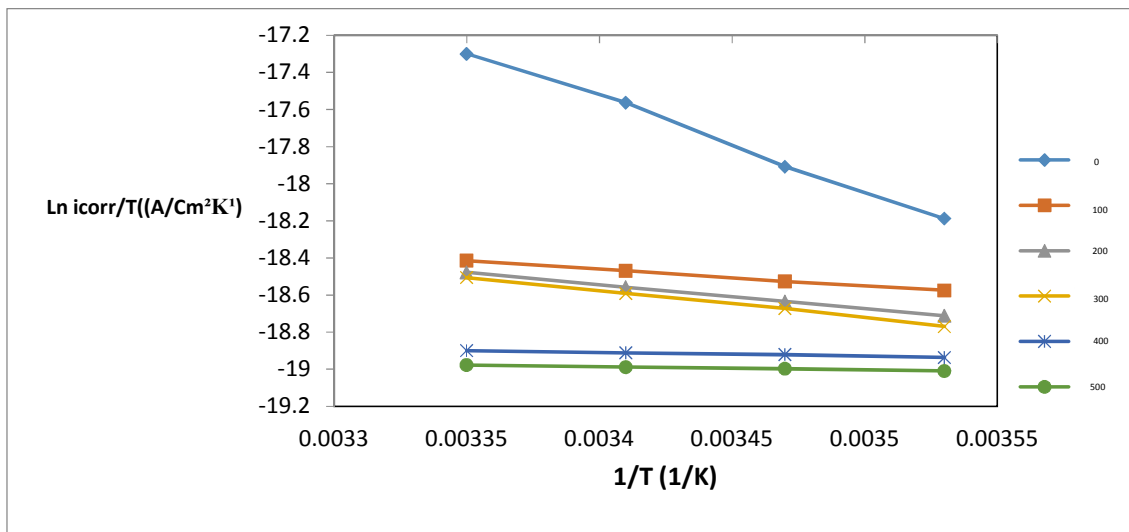


Figure 6. Transition state plots for 316 stainless steel. Solution containing 1 M HCl as well as: (a) 0, 100, 200, 300, 400, 500 ppm of 1-H-benzotriazole.

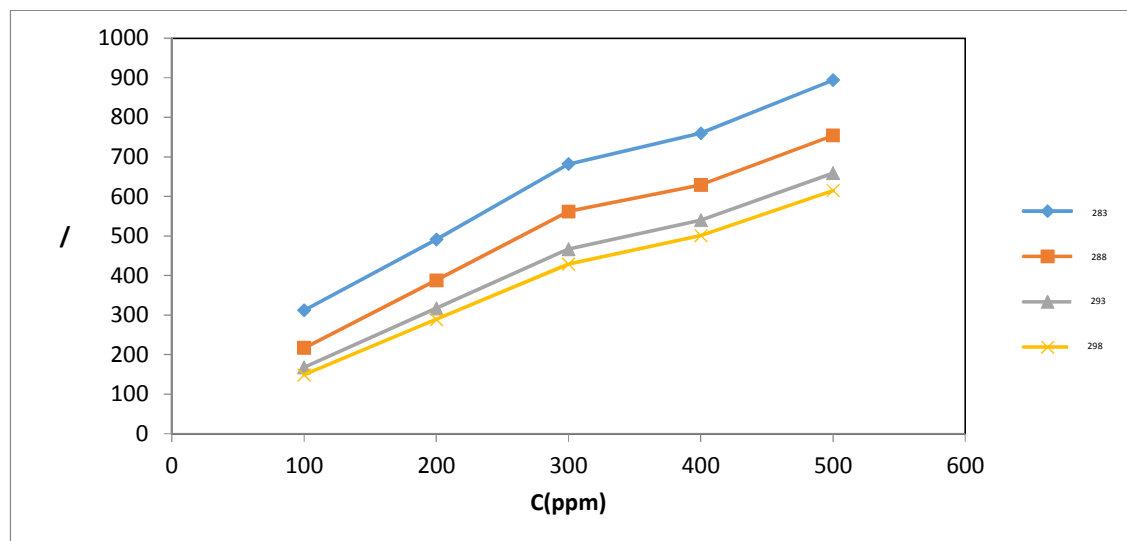


Figure 7. Adsorption isotherms of 1-H-benzotriazole on the 316 stainless steel in a 1 M HCl solution at different temperatures; 283, 288, 293, 298 °K.

After addition to corrosive solution 500ppm of 1-H-benzotriazole the energies of activation diminishes about twice only (Table 2). However, E_a does not change significantly which is characteristic for mixed type (physical and chemical) adsorption of 1-H-benzotriazole onto the SS surface. The positive signs the enthalpy of activation, ΔH_a reflect the endothermic process, which is attributable unequivocally to chemisorptions. Moreover, the enthalpy of chemisorptions process approaches 100 kJ mol^{-1} [32-34]. In the present study the ΔH_a value for 500ppm

of 1-H-benzotriazole was found 1.4 kJ mol^{-1} (Table 2) indicated that it is adsorbed onto the 316 stainless steel surface by both physical and chemical process.

The values of entropy activation, ΔS_a for different concentration of 1-H-benzotriazole are listed in Table 2. The large and negative values of ΔS_a imply that the activated complex in the rate determining step represents an association rather than a dissociation step, meaning that a decrease in disordering takes place on going from reactants to the activated complex.

Table 2. Corrosion kinetic parameters for 316 stainless steel in a 1 M HCl in the absence and presence of different concentrations of 1-H-benzotriazole.

| C ppm | E_a KJ mol^{-1} | ΔH KJ mol^{-1} | $-\Delta S$ $\text{J mol}^{-1} \text{K}^{-1}$ |
|-------|----------------------------|---------------------------------|---|
| Blank | 44.13 | 41.69 | 249.32 |
| 100 | 9.85 | 7.45 | 373.38 |
| 200 | 13.22 | 10.83 | 362.57 |
| 300 | 14.45 | 12.05 | 358.66 |
| 400 | 4.03 | 1.63 | 396.91 |
| 500 | 3.77 | 1.41 | 398.24 |

Adsorption parameters

The efficiency of organic molecules as good corrosion inhibitors mainly depends on their adsorption ability onto the metal surface. The inhibition efficiency is a function of the electrode surface covered by the inhibitor molecules. The degree of surface coverage for the 1-H-benzotriazole at different temperatures was depicted in Table 1. The adsorption isotherms can provide important clues to the nature of metal-inhibitor interaction it was established isotherms that describe the adsorptive behaviour of the inhibitor.

It was assumed that the adsorption of 1-H-benzotriazole onto the SS surface was described by the Langmuir isotherm [17, 30, 33]. The plot of 1-H-benzotriazole / θ vs. 1-H-benzotriazole yields straight lines, Figure 8 supporting the assumption that the adsorption of 1-H-benzotriazole from hydrochloric acid solutions onto the SS surface at the studied temperatures obeys a Langmuir adsorption isotherm which is represented by:

$$\frac{c_{inh}}{\theta} = \frac{1}{K_{ads}} + C_{inh} \quad (18)$$

Where 1-H-benzotriazole is the inhibitor concentration, K_{ads} is the equilibrium constant for the adsorption/desorption process.

From the intercepts of the straight lines on the 1-H-benzotriazole axis one can calculated,

K_{ads} values that relate the standard free energy of adsorption by:

$$\Delta G_{ads}^0 = -RT \ln (55.5 \times K_{ads}) \quad (19)$$

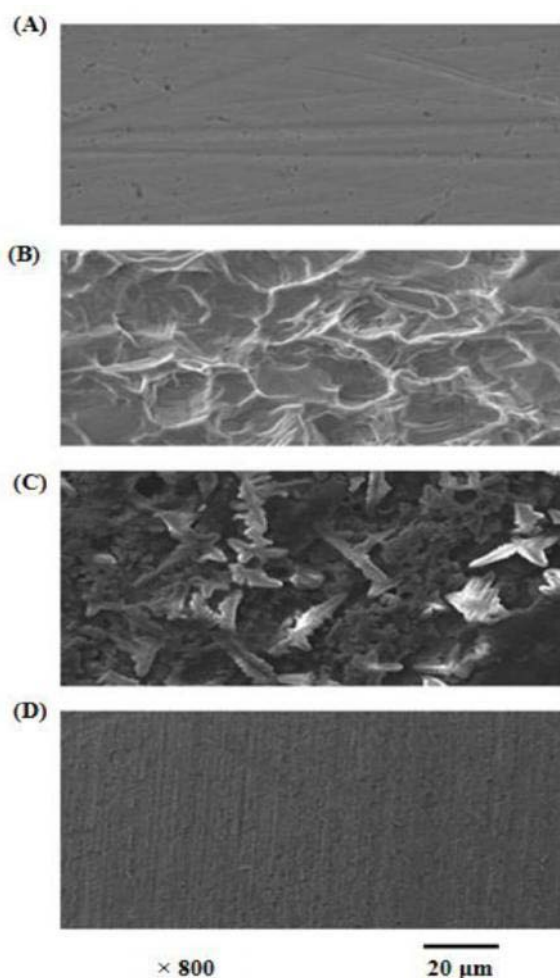


Figure 8. SEM micrographs of 316 stainless steel surface: (A) before immersion to solution of chlorides, (B) and (C) after exposition (24 hours) in a 1 M HCl solution or in the presence 500 ppm of 1-H-benzotriazole respectively, (D) after removal of the inhibiting film.

where the constant 55.5 is the molar process obtained from Langmuir adsorption concentration of water in solution. The isotherms for the studied inhibitor are given thermodynamic parameters for adsorption in Table 3.

Table 3. Slope of adsorption isotherm, linear correlation coefficient, equilibrium constant adsorption/desorption and standard free: energy, enthalpy, and entropy of the adsorption for 316 stainless steel in a 1 M HCl solution in the presence of 1-H-benzotriazole at different temperatures.

| temperatures $^{\circ}\text{K}$ | $K_{\text{ads}} \times 10^3$ M^{-1} | $-\Delta G_{\text{a}}$ KJ.mol^{-1} | ΔH_{a} KJ.mol^{-1} | ΔS_{a} KJ.mol^{-1} |
|------------------------------------|---|--|---|---|
| 263 | 7.14×10^2 | 24.91 | 13.85 | 136.96 |
| 268 | 7.69×10^2 | 25.52 | | 136.73 |
| 273 | 8.33×10^2 | 26.16 | | 136.57 |
| 283 | 9.09×10^2 | 26.82 | | 136.50 |

The absolute standard free energy of the adsorption values increase with temperature. The negative values of ΔG_{ads}^0 indicate spontaneous adsorption of 1-H-benzotriazole on the steel surface. The values of ΔG_{ads}^0 were changed in range from -24 to -26 kJ mol⁻¹ it is suggested that adsorption of Schiff base involves the physical and chemical adsorption of inhibitor onto the SS surface in hydrochloric acid solutions at the studied temperatures. Thermodynamically (ΔG_{ads}^0) is related to the standard enthalpy (ΔH_{ads}^0) and entropy (ΔS_{ads}^0) of the adsorption process according equation:

$$\Delta G_{ads}^0 = \Delta H_{ads}^0 - T\Delta S_{ads}^0 \quad (20)$$

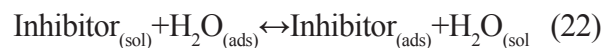
The standard enthalpy of adsorption can be calculated according to the Van't Hoff equation:

$$\ln K_{ads} = \frac{\Delta H_{ads}^0}{RT} \quad (21)$$

A plot of $\ln K_{ads}$ vs. $1/T$ gives straight line, as shown in Figure 9. The slope of the straight lines $-\Delta H_{ads}^0/R$. The value of standard free enthalpy of the adsorption is given in Table 3. Since the $-\Delta H_{ads}^0$ is positive this means that the adsorption of 1-H-benzotriazole the 316 stainless steel surface is an endothermic process, which is attributable unequivocally to chemisorptions [32-44].

The values of standard free entropy of the

adsorption are depicted in Table 3. The signs of ΔS_{ads}^0 are positive, values in the presence of inhibitor are large, and increased as compared to free acid solution. The adsorption of 1-H-benzotriazole from the aqueous solution can be regarded as substitution process between the inhibitor in the aqueous phase and water molecules onto the SS surface [35, 36]:



at present it is known that one adsorbed H₂O molecule is replaced by one of 1-H-benzotriazole molecule onto the 316 stainless steel surface. The substitution adsorption process may be exothermic, and the increase in entropy becomes the driving force for the adsorption of 1-H-benzotriazole on to the SS surface. The thermodynamic values obtained are the algebraic sum of adsorption of organic inhibitor molecule and desorption of water molecule.

Scanning electron microscopy studies

The surface morphology of stainless steel samples immersed in 1 M HCl solution for 24 hours in the absence and in the presence of 1-H-benzotriazole were studied by scanning electron microscopy. The solutions were not degassed.

Figure 8 show the surface morphology of 316 stainless steel specimens (A) before and (B) after being immersed in corrosive solution. The

photograph 8 (B) reveals that the surface was strongly damaged in absence of the inhibitor. Figure 8 (C) shows SEM image of SS surface after immersion (for the same time interval) in corrosive solution containing additionally 500ppm of 1-H-benzotriazole. The SEM photograph show that protective layer appears onto the surface of steel. The inhibitor film does not cover tightly the surface, and hence does not protect stainless steel surface to an adequate degree. The Figure 8 (D) presents sample after the removal of the inhibiting film. Chloride ions, oxygen and water penetrate the protective film through pores, flaws or other weak spots what results in the further corrosion of 316SS.

Conclusion

The inhibition effect of 1-H-benzotriazole on the corrosion of 316 stainless steel in chloride acid solutions was studied. From the data obtained the following points can be emphasized:

- The corrosion of 316SS in a 1 M HCl solution is significantly reduced by addition of 1-H-benzotriazole.
- The 1-H-benzotriazole behaves as mixed type corrosion inhibitor.
- Langmuir adsorption isotherm exhibited the best fit to the experimental data.
- The inhibition efficiency corrosion of SS increases with increase of concentration

of 1-H-benzotriazole, and in increase of temperature of solution.

- Thermodynamic activation parameters reflect the endothermic nature dissolution process of 316 SS.
- Thermodynamic adsorption parameters show that of 1-H-benzotriazole was adsorbed by spontaneous, endothermic process which is unequivocally to chemical adsorption of inhibitor.
- SEM micrographs showed that the 1-H-benzotriazole molecules form a protective film onto the SS surface.

References

- [1] O. A. Olsson, D. Landolt, *Electrochim. Acta*, 48, 1093 (2003).
- [2] M. Da Cunha Belo, M. Walls, N.E. Hakiki, J. Corset, E. Picquenard, G. Sagon, D. Noël, *Corros. Sci.*, 40, 447 (1998).
- [3] A. Yağan, N.Ö. Permez, A. Yıldız, *Corros. Sci.*, 49, 2905 (2007).
- [4] S. Şafak, B. Duran, A. Yurt, G. Türkoğlu, *Corros. Sci.*, 54, 251 (2012).
- [5] K. Emregül, O. Atakol, *Mater. Chem. Phys.* 83, 373 (2004).
- [6] U. Aytaç, Ü. Özmen, M. Kabasakaloğlu, *Mater. Chem. Phys.*, 89, 176 (2005).
- [7] M. Behpour, S.M. Ghoreishi, M. Salavati-Niasari, B. Ebrahimi, *Mater. Chem. Phys.*, 107, 153 (2008)
- [8] N. Soltani, M. Behpour, S.M. Ghoreishi, H. Naeimi, *Corros. Sci.*, 52, 1351 (2010).

- [9] M.G. Hosseini, S.F.L. Mertens, M. Ghorbani, M.R. Arshadi, *Mater. Chem. Phys.*, 78, 800 (2003).
- [10] A. Yurt, A. Balaban, S.U. Kandemir, G. Bereket, B. Erk, *Mater. Chem. Phys.*, 85, 420 (2004).
- [10] M. Lashgari, M.R. Arshdi, S. Miandari, *Electrochim. Acta*, 55, 6058 (2010)
- [11] Y.K. Agrawal, J.D. Talati, M.D. Shah, M.N. Desai, N.K. Shah, *Corros. Sci.*, 46, 633 (2004).
- [12] M. Behpour, S.M. Ghoreishi, N. Mohammadi, M. Salavati-Niasari, *Corros. Sci.*, 53, 3380 (2011).
- [13] M. Behpour, S.M. Ghoreishi, N. Soltani, M. Salavati-Niasari, *Corros. Sci.*, 51, 1073 (2009).
- [14] C. Küstü, K.C. Emregül, O. Atakol, *Corros. Sci.*, 49, 2800 (2007).
- [15] H.D. Leçe, K.C. Emregül, O. Atakol, *Corros. Sci.*, 50, 1460 (2008).
- [16] M.G. Hosseini, M. Ehteshamzadeh, T. Shahrabi, *Electrochim. Acta*, 52, 3680 (2007)
- [17] R.A. Prabhu, T.V. Venkatesha, A.V. Shanbhag, G.M. Kulkarni, R.G. Kalkhambkar, *Corros. Sci.*, 50, 3356 (2008).
- [18] K.S. Jacob, G. Parameswaran, *Corros. Sci.*, 52, 224 (2010).
- [19] I. Ahamad, R. Prasad, M.A. Quraishi, *Mater. Chem. Phys.*, 124, 1155 (2010).
- [20] M.A. Hegazy, M.F. Zaky, *Corros. Sci.*, 52, 1333 (2010).
- [21] P.C. Okafor, Y. Zheng, *Corros. Sci.*, 51, 850 (2009).
- [22] I.B. Obot, N.O. Obi-Egbedi, S.A. Umoren, *Corros. Sci.*, 51, 1868 (2009).
- [23] Z. Begum, A. Poonguzhali, R. Basu, C. Sudha, H. Shaikh, R.V. Subba Rao, *Corros. Sci.*, 53, 1424 (2011).
- [24] I.O.M. Bockris, B. Young, *J. Electrochem. Soc.*, 139, 2237 (1991).
- [25] N.E. Hakiki, *Corros. Sci.*, 53, 2688 (2011).
- [26] M.S.S. Morad, A.A.A. Hermas, *J. Chem. Technol. Biotechnol.*, 76, 401 (2001).
- [27] W. Li, Q. He, S. Zhang, C. Pei, B. Hou, *J. Appl. Electrochem.*, 38, 289 (2008).
- [28] F.G. Liu, M. Du, J. Zhang, M. Qiu, *Corros. Sci.*, 51, 102 (2009).
- [29] A.Y. Musa, A.A.H. Kadhum, A.B. Mohamad, M.S. Takriff, A.R. Daud, S.K. Kamarudin, *Corros. Sci.*, 52, 526 (2010).
- [30] A.Y. Musa, A.A.H. Kadhum, A.B. Mohamad, M.S. Takriff, *Mater. Chem. Phys.*, 129, 660 (2011).
- [31] S. Martinez, I. Stern, *Appl. Surf. Sci.*, 199, 83 (2002).
- [32] A.K. Singh, M.A. Quraishi, *Corros. Sci.*, 51, 2752 (2009).
- [33] A.K. Singh, M.A. Quraishi, *Corros. Sci.*, 52, 152 (2010).
- [34] M. Şahin, S. Bilgiç, H. Yılmaz, *Appl. Surf. Sci.*, 195, 1 (2002).
- [35] J. Trela, M. Scendo, *Corrosion Protection*, 55, 86 (2012).
- [36] S. Ramachandran, B.L. Tsai, M. Blanco,

- H. Chen, Y. Tang, W.A. Goddard, *J. Phys. Chem. A*, 101, 83 (1997).
- [37] I. Lukovits, K. Palfi, E. Kalman, *Corrosion*, 53, 915 (1997).
- [38] E.H. El-Ashri, A. El-Nemr, S.A. Essawy, S. Ragub, *Electrochim. Acta*, 51, 3957 (2006).
- [39] N.O. Obi-Egbedi, I.B. Obot, *Corros. Sci.*, 53, 263 (2011).
- [40] S.E. Nataraja, T.V. Venkatesha, K. Manjunatha, B. Poojary, M.K. Pavithra, H.C. Tandon, *Corros. Sci.*, 53, 2651 (2011).
- [41] H. Ju, Z. Kai, Y. Li, *Corros. Sci.*, 50, 865 (2008).
- [42] A.Y. Musa, A.A.H. Kadhum, A.B. Mohamad, A.A.B. Rahoma, H. Mesmari, *J. Mol. Struct.*, 969, 233 (2010).
- [43] M. Scendo, J. Trela, N. Radek, *Corros. Rev.*, 30, 33 (2012).